Colloid Polym Sci (2006) 285:273–281
DOI 10.1007/s00396-006-1560-1

ORIGINAL CONTRIBUTION

Synthesis and characterization of a functionalized amphiphilic diblock copolymer: MePEG-*b*-poly(DL-lactide-*co*-RS-β-malic acid)

Liang Wang · Xiaohua Jia · Xiaohang Liu · Zhi Yuan · Jiaxian Huang

Received: 31 December 2005 / Accepted: 22 May 2006 / Published online: 28 September 2006

Abstract A class of novel amphiphilic diblock copolymer of MePEG-*b*-poly(DL-lactide-*co*-RS-β-malic acid) has been synthesized via the hydrogenation over palladium on charcoal of MePEG-*b*-poly(DL-lactide-*co*-RS-*β*-benzyl malolactonate), which was prepared by ring-opening copolymerization of DL-lactide and RS-β-benzyl malolactonate (MABz) using methyl-polyethylene glycol (MePEG) as the initiator and stannous octoate as the catalyst. The influence of copolymerization temperature, reaction time, macro-initiator (MePEG-5000) proportion and monomer ratio was studied. Gel permeation chromatography measurements revealed that the molecular weight decreased with increasing MABz feeding dose. The configurational structures of the protected and de-protected copolymers were determined by ^{13}C nuclear magnetic resonance (NMR), ^{1}H NMR and Fourier transform infrared. A water-swollen core of the nanospheres formed from the de-protected copolymer was discovered by transmission electron microscopy measurement. Additionally, the degradation experiments indicated that more hydrophilic malic acid content led to higher degradation rate.

Keywords MePEG-*b*-poly(DL-lactide-co-RS-β-malic acid) · MePEG-*b*-poly(DL-lactide-co-RS-β-benzyl malolactonate) · Hydrogenolysis · Nanosphere · Degradation

L. Wang · X. Jia · X. Liu · Z. Yuan (✉) · J. Huang
Key Laboratory of Functional Polymer Materials,
Ministry of Education, Institute of Polymer Chemistry,
Nankai University, Tianjin 300071, China
e-mail: zhiy@nankai.edu.cn

Introduction

Biodegradable functional polymers are attractive materials in biomedical areas. The availability of strategically placed functional groups facilitates covalent prodrug attachment as well as other functionalizations [1–5]. By derivation of the pendant functional groups, variations in hydrophilicity, physical properties and biodegradability can be achieved [6, 7].

Materials composed of poly(lactic acid) (PLA) have gained wide acceptability for applications that require bioresorption in vivo [8–10]. The degradation rate of PLA-based polymeric materials is a function of hydrophilic/hydrophobic properties. Strategies to regulate this factor have involved copolymerizations of DL-lactide (DLLA) with glycolide [11], ethylene oxide [12–15], ε-caprolactone [16] and monomers that, upon ring opening, provide amino acid repeat units [17–19]. Also, many workers have attempted to "tailor" PLA physical property and hydrolytic degradability by blending PLA with other polymers [20].

Kumar et al. [21] prepared copolymers of L-lactide-co-pentofuranose, and then selectively removed the ketal-protecting groups or benzyl-protecting groups to give vicinal diol or hydroxyl pendant groups. He et al. [23] prepared poly(L-lactic acid-*co*-RS-β-malic acid) [22], which was applied to tissue-engineering carrier.

As for drug delivery systems, micelles formed from amphiphilic block copolymers have recently attracted significant attention in the diverse field of medicine and biology. In particular, polymeric micelles have been developed as a drug and gene delivery system [24–26], as well as carriers for various contrasting agents in diagnostic imaging applications [27]. In an aqueous solution, the hydrophobic blocks of the copolymer are expected to

segregate into the core of the micelle, whereas the hydrophilic blocks form the corona or outer shell. Such core-shell architecture of the polymeric micelles is essential for their utility as novel functional materials for pharmaceutical applications. The hydrophobic micelle core serves as a microenvironment for the incorporation of various therapeutic compounds; the corona, or outer shell, serves as a stabilizing interface between the hydrophobic core and the external medium. As a result, polymeric micelles can be used as efficient containers for reagents with poor solubility and/or low stability in physiological environments [28, 29]. PEG-*b*-PLA diblock copolymers are widely used as the micelle materials because of their non-toxicity and biocompatibility [30–33]. Usually, a hydrophobic drug was loaded in the micelle core, released during the degradation of the micelle. But this micelle was not suitable for a hydrophilic drug, such as a hydrophilic protein drug.

In order to solve this problem, our work was carried out to synthesize PEG-*b*-PDLLA diblock copolymers with hydrophilic pendant groups in poly-DL-lactide (PDLLA) segment. Polyesters with pendant carboxylic and amino functional groups, such as poly(malic acid) (PMA) [34, 35] and poly(L-serine ester) [36, 37], are already obtained. In this paper, malic acid (MA) was introduced into the PDLLA block of PEG-*b*-PDLLA by the ring-opening copolymerization of DLLA and RS-β-benzyl malolactonate (MABz), which was initiated by the hydroxyl end group of MePEG-5000. The relationship between the reaction parameters and the molecular weight (Mw) of MePEG-*b*-poly(DLLA-*co*-RS-β-MABz) was established, and the optimum reaction condition was found out. The successful removal of benzyl protective groups was proved by nuclear magnetic resonance (NMR) and Fourier transform infrared (FTIR) measurement. The nanospheres formed from the protected and the de-protected copolymers were investigated through transmission electron microscopy (TEM) measurement, and the degradation of the copolymer films was also studied in vitro.

Materials and methods

Materials

Stannous octoate, trifluoroacetic acid anhydride (TFAA), palladium on charcoal (Pd/C) and MePEG-5000 were purchased from Aldrich and were used without further purification. Solvents such as tetrahydrofuran (THF), 1,4-dioxane and ethyl ether were dried with sodium and distilled. Acetonitrile and dichloromethane were dried with CaH_2 and distilled. Benzyl alcohol was distilled. DLLA was purchased form Beijing Chemical Reagent Company and was recrystallized twice in acetyl acetate.

Synthesis of diblock copolymers

Synthesis of RS-β-benzyl malolactonate

(*RS*)-Bromosuccinic acid was prepared and purified starting from aspartic acid according to the literature [38]. Briefly, 100 g of DL-aspartic acid and 426 g (5.5 Eq, 4.13 mol) of NaBr were dissolved in 1,600 ml of 2 mol/l H_2SO_4. Sixty-two grams (1.2 Eq, 0.9 mol) of $NaNO_2$ was added to the solution. The mixture was stirred for 30 min. Eight grams of urea was added. The aqueous phase was extracted by ethyl acetate. The organic phase was dried over $MgSO_4$/decolorizing charcoal for 1 h. After filtration, the solvent was eliminated to give yellow powder. Pure (*RS*)-bromosuccinic acid was obtained by twice recrystallization in acetonitrile.

Ten grams (0.05 mol) of *RS*-bromosuccinic acid, which was previously dried under vacuum, was dissolved in 20 ml THF under N_2 atmosphere. Then, the mixture was stirred vigorously in ice bath, and 10 ml (0.07 mol) of TFAA was added gradually. When the mixture became clear, it was kept stirring at room temperature for 2 h. Then the solvent was evaporated under vacuum, and a kind of pale yellow oil was obtained. Pale yellow oil (15 g) was suspended in 50 ml of distilled water and 25 ml of dioxane. A solution of 2 mol/l NaOH was added dropwise into the mixture until the pH reached 7.2. Then 150 ml of benzene was added into the solution, and the mixture was stirred vigorously at 45 °C for 3 h. After decantation, the organic phase was washed with 5% $NaHCO_3$ aqueous solution, slightly acid water and water, in turn, until neutrality, and then it was dried over $MgSO_4$. After filtration, the benzene was eliminated under vacuum, and 3.9 g of crude lactone was obtained. Pure lactone (2.4 g) was obtained with 11.68% yield by twice chromatography on silica gel (eluent: dichloromethane/petroleum ether, 9:1).

Copolymerization

Prescribed amounts of DLLA, RS-β-MABz and MePEG-5000 and 0.1 wt.% stannous octoate were put into a polymerization tube. Then, the tube was replaced by nitrogen and heated to 80 °C under vacuum to remove oxygen and trace water. The polymerization tube was sealed under vacuum and placed into an oil bath. After copolymerization, the resulting copolymer was dissolved in ethyl acetate and was precipitated into a large amount of petroleum ether. The white deposit of MePEG-*b*-poly(DLLA-*co*-RS-β-MABz) was dried under vacuum at 45 °C for 2 days.

Removal of protective groups

Pd/C (0.2 g) was added into a solution of 1.0 g of MePEG-*b*-poly(DLLA-*co*-RS-β-MABz) in 100 ml of 1,4-dioxane

and 10 ml of acetone. This system was stirred continuously and bubbled with hydrogen for 24 h. Then, Pd/C was filtered off and washed with acetone. The filtrate was evaporated, and the thickened solution was poured into a large amount of petroleum ether to give the de-protected copolymer as white solid. The white precipitate was dried under vacuum at 45 °C for 2 days (yield=98%).

Preparation of the nanospheres

Suspensions of nanosphere formed from the protected and de-protected copolymers were prepared by the solvent evaporation method. Briefly, 10 mg of the copolymer was dissolved in 2 ml of acetone, and this solution was added dropwise into 10 ml of distilled water under vigorous stir. Then, the obtained suspension was agitated by a magnetic stirrer at room temperature until complete evaporation of the organic solvent had taken place. The nanosphere suspensions used in the TEM measurement were freshly prepared.

In vitro degradation experiment

Fifty milligrams of the de-protected copolymer was dissolved in 2 ml of acetone in a glass plate with 1.5-cm diameter. After the solvent was evaporated, 2 ml of 0.2 mol/l phosphate buffer solution (PBS, pH 7.4) were added. And then the system was kept at 37.0±0.5 °C in a shaking bath. After each degradation period, the samples were washed with distilled water and dried in a vacuum oven at 40 °C for 24 h and weighed. The weight-loss percentages of these samples were calculated from the weights of dry sample obtained before and after degradation.

Measurement

^{1}H and ^{13}C NMR spectra were recorded on a Bruker DMX-300 with tetramethylsilane as the internal standard and $CDCl_3$ as the solvent. FTIR spectra were recorded on FTS-6000 spectrometer. Gel permeation chromatography (GPC) was performed on Waters 515 with Polymer Standards Service Columns. Samples were measured at 35 °C with THF as eluent at a flow rate of 1.0 ml/min. The Mw was calibrated by the polystyrene standards. Nanosphere morphology was characterized by a JEM-2010F electron microscope. Samples for the microscopy were dry.

Results and discussion

The aim of this work was to functionalize the PDLLA block of MePEG-*b*-PDLLA. RS-β-MABz, which would introduce carboxyl groups into PDLLA block, was selected to copolymerize with DLLA. Possible initiation mechanism of this copolymerization was coordination–insertion [39, 40]. The synthesis of RS-β-MABz was presented in Materials and Methods, and the synthetic route of MePEG-*b*-poly(DLLA-*co*-RS-*β*-MA) is shown in Scheme 1.

Copolymerization

First of all, the effects of temperature were studied with 9.27 mol% MABz content in the monomer feed. The content of stannous octoate and methyl-polyethylene glycol (MePEG) was 0.1 and 11.2 wt.%, respectively. The reaction time was 48 h. The Mw of the copolymer with reaction temperature variation is listed in Table 1. It revealed that the yields (>85%) of copolymers were high when the temperature was above 130 °C; otherwise, the yield (75.3%) was low at 120 °C. Since the melting point of DLLA was 127 °C and it was unable to melt at a temperature as low as 120 °C, it was hard for the DLLA monomer to copolymerize with the MABz monomer. The Mw of the copolymer increased with increasing temperature when the temperature was below 140 °C and decreased when the temperature further increased because more chain transfer reaction occurred at the higher temperature. In this series, the Mws of the copolymer synthesized at 120, 130, 140, 150 °C were 12,900, 15,100, 10,100 and 8,900, respectively. Both of the highest Mw and yield of the copolymers were observed at 130 °C, and further studies were all carried out at 130 °C.

The composition variations of copolymers with 18.7 mol% MABz in the monomer feed during the copolymerization process are shown in Table 2. When the copolymerization time was 6, 24, 48 and 96 h, the content of MABz in the copolymer was 8.7, 12.9, 17.6 and 17.6%, respectively. The content of MABz increased with increasing time within 48 h. It demonstrated that the reactivity of DLLA was higher than that of RS-β-MABz. According to the literature [41], the stereoelectronic effect of the four-

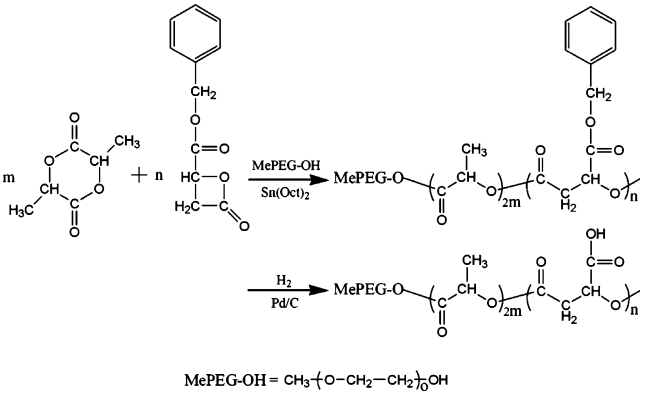

Scheme 1 Synthetic route of MePEG-b-poly(DLLA-*co*-RS-β-MA)

Table 1 Molecular weight of the protective copolymers with the copolymerization temperature varied from 120 to 150 °C[a]

Copolymer	Temp. (°C)	MABz content (mol%)			Mw of copolymer[b]		
		Feeding	Polymer[c]	Yield (%)	Mn	Mw	Mw/Mn
A	120	9.27	6.38	75.3	7,700	12,900	1.67
B	130	9.27	8.84	95.2	8,500	15,100	1.77
C	140	9.27	6.52	90.2	6,100	10,100	1.64
D	150	9.27	5.74	85.6	5,700	8,900	1.54

[a] Copolymerized for 48 h with 11.9 wt.% MePEG initiator, 9.27% MABz feeding and 0.1 wt.% catalyst
[b] Determined by GPC
[c] Calculated from ^{1}H NMR

member ring monomer of MABz was the main reason, and the stereo hindrance of benzyl protective group also contributed to the low reactivity of MABz. The slight broadening of polydispersity was observed as reaction time extended. The transesterification of the polymer chains, which commonly occurred in the ring-opening polymerization, could be the reason of this observation. In Table 2, it was obviously suggested that the suitable polymerization time was 48 h, and longer reaction time would reduce the Mw.

Furthermore, the copolymerization reactions with various monomer feeds were investigated. Table 3 showed that the Mw of the copolymer decreased with increasing MABz feeding dose. The Mw of the MPEG-*b*-PDLLA prepared at the same condition was 32,500, but it was reduced by nearly half when MABz was added. The Mws of the copolymers with 9.27, 18.7, 27.7 and 38.0 mol% MABz content were 15,100, 11,500, 9,700 and 8,000, respectively, and the Mw of the copolymer with 100 mol% MABz feeding dose was only 6,100. The yields of these copolymerization reactions decreased from 98.1 to 60.0% as the MABz content increased from 0 to 100%. The polymerization of DLLA is a reversible process, and the equilibrium monomer concentration increased with increasing temperature. MABz repeat units were likely more reversible to monomer than DLLA units, which might result in lower yields and Mw of MePEG-*b*-poly(DLLA-*co*-MABz) than those of MePEG-*b*-poly(DLLA).

Studies were also carried out on the copolymerization with different initiator feeds. With the temperature maintained at 130 °C for 48 h, the polymerizations were initiated by variable MePEG contents. Table 4 showed that the Mw of the copolymer increased as the MePEG content decreased. But the Mw was not equal to the ratio of monomer and initiator as we expected. It might be that low-level impurities of benzyl alcohol or water were present along with MABz. If so, both of these impurities might initiate chains and contribute to reduced Mw values for copolymers.

Therefore, the decrease of Mw was the result of all the influential factors presented above, such as low-level impurities of MABz and transesterification. GPC traces of the copolymers with MePEG content variations are shown in Fig. 1. The molecular distribution of the copolymer became relatively narrow with increasing MePEG content in the feeding dose, and single peak was found in each GPC curve.

Hydrogenolysis

Hydrogenation using Pd/C as the catalyst is a useful and mild method for the removal of the benzyl ester group. Work was performed to determine a preferable solvent for

Table 2 Molecular weight of the protected copolymer with different copolymerization time[a]

Copolymer	Reaction time (h)	MABz content (mol%)			Mw of copolymer[b]		
		Feeding	Polymer[c]	Yield (%)	Mn	Mw	Mw/Mn
E	6	18.7	8.7	60	3,800	6,349	1.64
F	24	18.7	12.9	79	4,800	8,000	1.67
G	48	18.7	17.6	92	6,100	11,500	1.90
H	96	18.7	17.6	94	5,700	11,300	1.96

[a] Copolymerized at 130 °C with 11.9 wt.% MePEG initiator, 18.7% MABz feeding and 0.1 wt.% catalyst
[b] Determined by GPC
[c] Calculated from ^{1}H NMR

Table 3 Molecular weight of the protected copolymer with monomer feed variation[a]

Copolymer	MABz content (mol%)			Mw of copolymer[b]		
	Feeding	Polymer[c]	Yield (%)	Mn	Mw	Mw/Mn
I	0	0	98.1	16,500	32,500	1.96
J	9.27	8.84	95.2	8,500	15,100	1.77
K	18.7	17.6	92.6	6,100	11,500	1.90
L	27.7	25.2	88.4	5,500	9,700	1.75
M	38.0	37.8	79.1	4,800	8,000	1.67
N	100	100	60.0	4,000	6,100	1.53

[a] Copolymerized at 130 °C for 48 h with 11.9 wt.% MePEG initiator and 0.1 wt.% catalyst
[b] Determined by GPC
[c] Calculated from ^{1}H NMR

this reaction. Ethyl acetate, acetone and THF were examined. Debenzylation performed in these solvents was slow. Even though MePEG-*b*-poly(DLLA-*co*-MABz) was highly soluble in chloroform, dichloromethane and toluene, debenzylation reactions in these solvents were unsuccessful. Fortunately, the mixed solvent of acetone and 1,4-dioxane was effective, and a high degree of debenzylation (above 95%) was achieved in this solvent.

Figure 2 showed ^{1}H NMR spectra of the protected and the de-protected copolymer. Compared with the ^{1}H NMR spectra of MPEG-*b*-PDLLA and MPEG-*b*-PMABz, the signals at 1.57 and 5.17 ppm were attributed to the CH_3 (4) and C*H* (3) protons of DLLA repeated units, respectively. The signals at 5.50 and 2.90 ppm were the C*H* (6) and CH_2 (5) protons of MABz repeated units in the copolymer main chain. The signals at 5.09 and 7.34 ppm were protons of pendant groups CH_2 (7) and benzene ring C$_6H_5$ (8). The signal at 3.71 ppm was CH_2 (1, 2) proton in the MePEG block. The chemical shifts of C*H* (3) in DLLA and CH_2 (7) in the pendant groups of MABz units were very close, and both of them were multi-peaks, so the peaks from 5.09 to 5.17 ppm were complex. Since the MABz units were low-content component in the copolymer, they were separated by a large amount of DLLA repeat units; the proton signals of MABz units were a little wider than that of DLLA units, especially the signals at 5.50 and 2.90 ppm of C*H* (6) and CH_2 (5) protons. After hydrogenolysis, the proton signal of C$_6H_5$ (8) in the pendant groups at 7.34 ppm was extremely weakened. The degree of debenzylation was calculated by monitoring the extent of decrease of the phenyl group protons C$_6H_5$ (8) at 7.34 ppm relative to proton C*H* (6) at 5.92 ppm.

The full ^{13}C NMR spectra of the protected and de-protected copolymers were displayed in Fig. 3. Assignments of the major resonances were based on the spectra of poly(L-lactide) and PMA homopolymers [42–45]. The signals at 16.9, 69.1 and 169.5 ppm were assigned to the *C*H$_3$ (4), *C*H (3) and *C*O (2) in the DLLA repeated units. The signals at 169.0, 35.3 and 67.2 ppm were due to the *C*O (5), *C*H$_2$ (6) and *C*H (7) of MABz units in the copolymer main chain. The signals at 168.0 and 69.4 ppm were attributed to the *C*O (8) and *C*H$_2$ (9) in the pendant groups. The signals from 135.0 to 128.2 ppm were the benzene ring (*C*$_6$H$_5$) (10), and the single peak at 70.5 ppm was the contribution of *C*H$_2$ (1) of MePEG. After hydrogenolysis, the signals of the benzyl groups (*C*$_6$H$_5$) (10) at 135.0–128.2 ppm and *C*H$_2$ (9) at 69.4 ppm disappeared. It also indicated the removal of the protective benzyl groups.

Table 4 Molecular weight of the protected copolymer with different contents of MePEG[a]

Copolymer	MePEG content (wt.%)		MABz content (mol%)			Mw of copolymer[b]		
	Feeding	Polymer[b]	Feeding	Polymer[c]	Yield (%)	Mn	Mw	Mw/Mn
O	6.30	8.09	9.27	6.23	82.3	8,400	16,100	1.91
P	9.16	9.70	9.27	8.68	87.4	8,700	16,700	1.93
Q	11.9	12.6	9.27	8.84	95.2	8,500	15,100	1.77
R	16.8	17.4	9.27	8.69	96.9	8,700	14,800	1.70
S	21.2	23.4	9.27	7.77	96.6	8,800	13,200	1.50

[a] Copolymerized at 130 °C for 48 h with 9.27% MABz feeding and 0.1 wt.% catalyst
[b] Determined by GPC
[c] Calculated from ^{1}H NMR

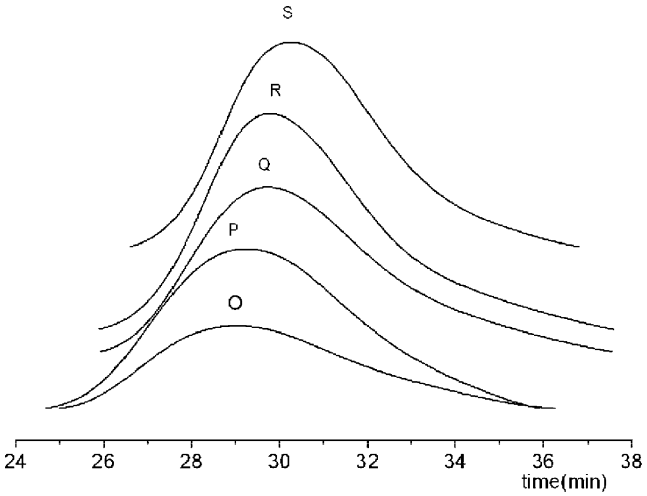

Fig. 1 GPC curves of the protected copolymer with different MePEG contents

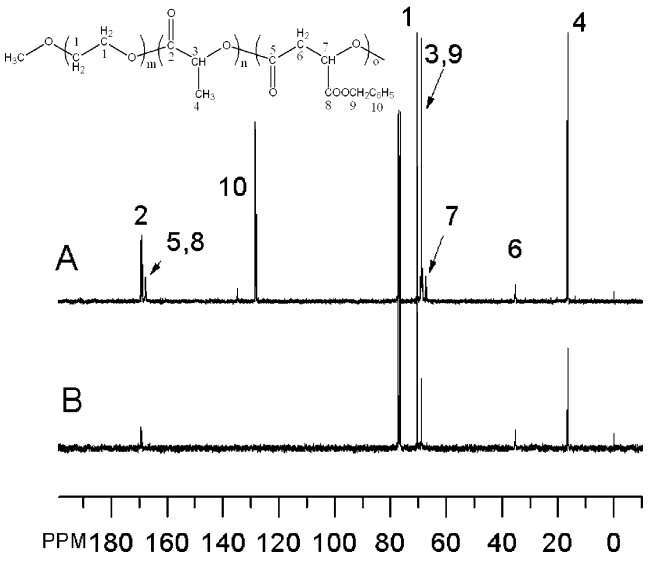

Fig. 3 ^{13}C NMR spectra of the copolymers (J): **a** the protected copolymer; **b** the de-protected copolymer: $CDCl_3$ as solvent

The ^{13}C NMR spectra at carbonyl region were relatively complicated, so that the amplificatory spectra were used to see the specific difference between the protected and the de-protected copolymers. Comparing the two spectra in Fig. 4, it could be seen that the signal at 169.5, 169.0 and 169.3 ppm still existed, but the signal at 168.0 ppm disappeared, whereas a new signal at 171.3 ppm appeared after the de-protection. So the signals at 169.5, 169.3 and 169.0 ppm were assigned to the *C*O in the copolymer main chain; the signal that disappeared at 168.0 ppm was the *C*O of pendant carbonyl groups in the protected copolymer; and the new signal that appeared at 171.3 ppm was the *C*O of pendant carboxyl groups in the de-protected copolymer. The peak (5) that was attributed to the *C*O of MABz units in the copolymer main chain was multiple and broad. The neighboring peaks were shoulders of the peak (5) that were likely due to sequence effects. For example, these peaks might arise as a result of L*M* and M*M* sequences (L=DLLA units, M=MABz units). So, the random structure of poly (DLLA-*co*-MABz) block was confirmed.

The FTIR spectra of the protected and the de-protected copolymers were shown in Fig. 5. After hydrogenolysis, the CH vibration of benzene at 700 and 752 cm^{-1} weakened remarkably. However, the OH vibration at 3,445 cm^{-1} strengthened greatly in the de-protected copolymer. These results further confirmed the removal of the benzyl group. Normally, once the benzyl protective group was removed, the Mw of the copolymer should decrease. On the contrary, the Mw increased a little. The Mw of the protected and de-protected copolymers (K) were 11,500 and 12,700, respectively. The

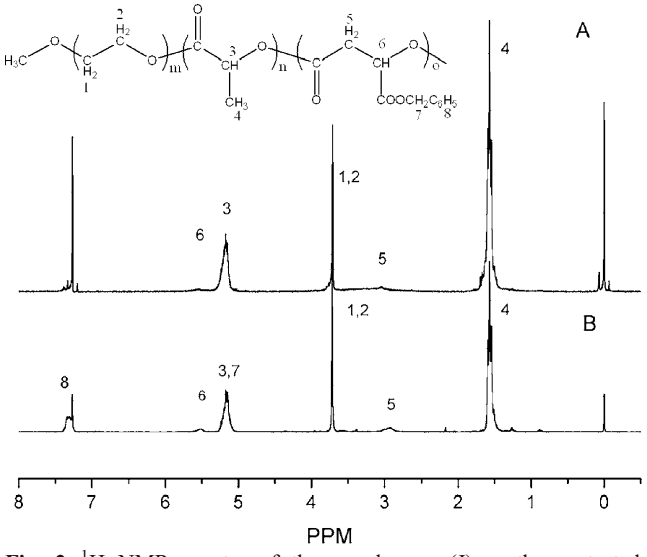

Fig. 2 ^{1}H NMR spectra of the copolymers (J): **a** the protected copolymer; **b** the de-protected copolymer: $CDCl_3$ as solvent

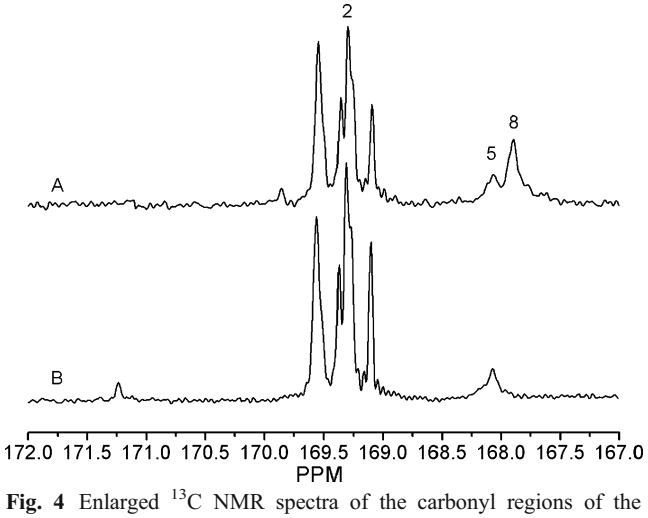

Fig. 4 Enlarged ^{13}C NMR spectra of the carbonyl regions of the copolymers (J): **a** the protected copolymer; **b** the de-protected copolymer: $CDCl_3$ as solvent

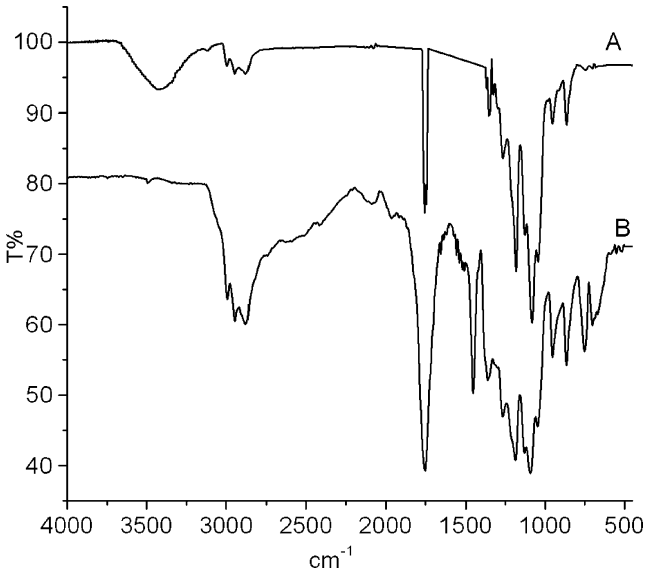

Fig. 5 FTIR spectra of the protected and the de-protected copolymers (K): **a** the de-protected copolymer; **b** the protected copolymer

inter- or intra-molecular hydrogen bond formed by the pendant carboxyl group led to the increase of the Mw.

Morphological characterization of the nanospheres formed by the protected and the de-protected copolymer

The protected and de-protected copolymers (K) were employed to prepare the nanosphere suspensions. A series of transmission electron micrograph of nanospheres formed from the protected copolymer and the de-protected copolymer was shown in Fig. 6.

Comparing Fig. 6a with Fig. 6b, the size of the nanosphere formed from the protected copolymer was larger than that from the de-protected copolymer. It also could be seen from the enlarged TEM pictures (Fig. 6b and d) that the nanospheres of the protected copolymer had a compact structure, while the nanospheres of the de-protected copolymer had an incompact structure. The different morphologies of the nanospheres were the contribution of the different structures between the protected and de-protected copolymer. Poly(DLLA-*co*-MA) block of the de-protected copolymer was water-insoluble but water-swollen, so the incompact structure was found among these nanospheres. Since the nanospheres for the TEM observation were air-dried, the water-swollen nanospheres formed from the de-protected

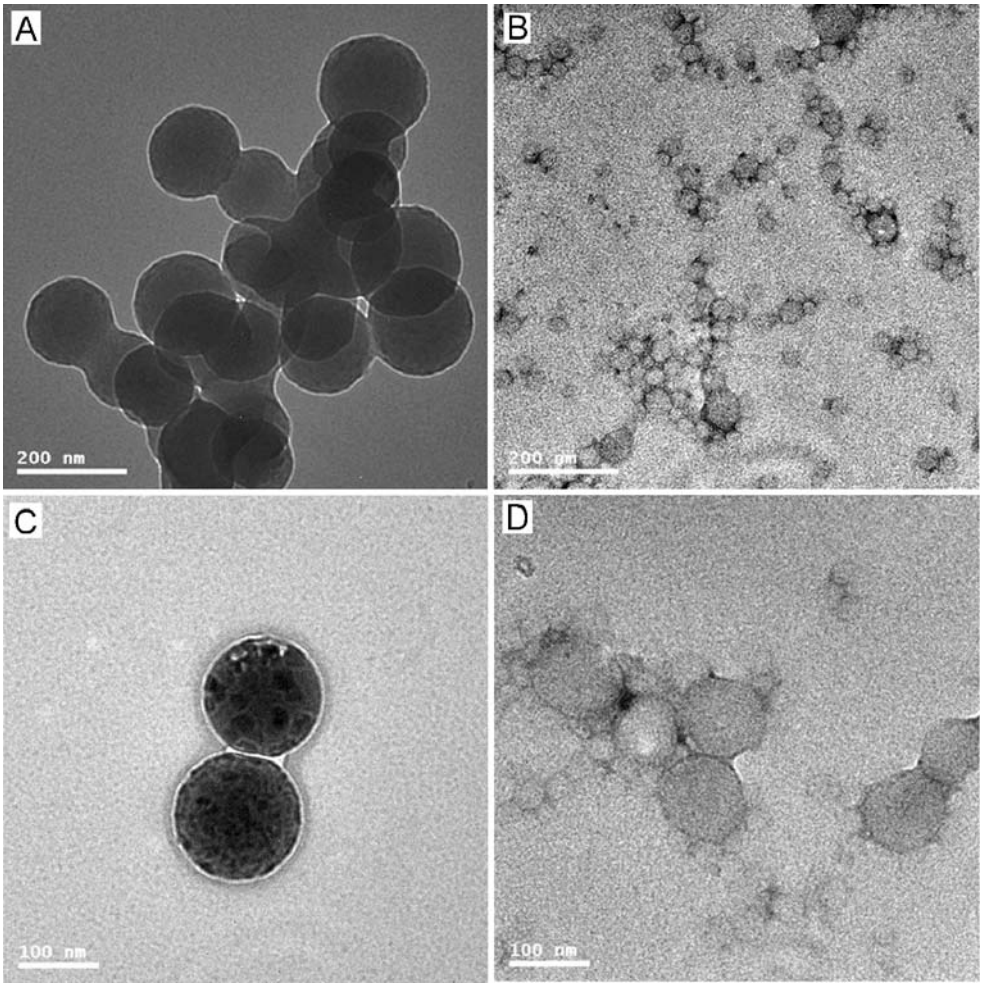

Fig. 6 TEM pictures of the nanospheres formed from the copolymer (K): **a**, **c** the nanospheres formed from the protected copolymer; **b**, **d** the nanospheres formed from the de-protected copolymer

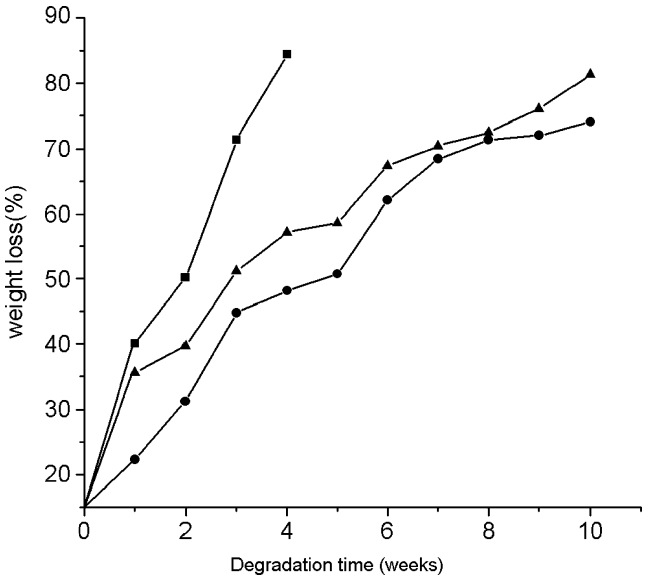

Fig. 7 Weight loss of the de-protected copolymers (J, K and L) during degradation in pH 7.4 PBS solution at 37 °C: J (*filled circle*); K (*filled triangle*); L (*filled square*)

copolymer might shrink more than those formed from the protected copolymer. So the size of these water-swollen nanospheres was smaller as displayed on the TEM pictures.

In vitro degradation experiment

Weight-loss data were obtained by the following equation:

$$\text{Weight loss}\,(\%) = (W_0 - W_d)/W_0$$

where W_0 is the initial weight of the samples, and W_d is the weight of the samples during different degradation periods. Figure 7 showed the weight loss of copolymer (J, K and L) according to the degradation time. In order to get a full trend of each curve, all the weight-loss curves started from the zero point. The de-protected copolymer (L) lost its weight so rapidly that the weight loss reached 87% after 4 weeks. For the de-protected copolymers (J and K), weight-loss percentages increased continuously to 72 and 81% in 10 weeks. It was found that the hydrophilicity–hydrophobicity balance played an important role in the degradation of the MePEG-*b*-poly(DLLA-*co*-RS-β-MA) copolymers so that the degradation rate increased with increasing hydrophilic MA content. There were two fast degradation periods of copolymers (J and K) in the whole weight-loss process. One was the beginning 3 weeks; the other was the sixth week and the seventh week. Because water was easily diffused into the polyester units, which linked to the water-soluble MePEG block, these polyester units could degrade firstly in the beginning 3 weeks. Similarly, the MA units could degrade firstly due to its high hydrophilicity. However, in the first 5 weeks, the hydrophobic PDLLA segments degraded very slowly. Since the sixth week, the degradation of PDLLA segments speeded up.

Conclusions

The copolymerization of DLLA and RS-β-MABz initiated by the macro initiator of MePEG-5000 was performed in bulk using stannous octoate as catalyst. The effects of copolymerization temperature, reaction time, monomer ratios and initiator contents were studied. It could be concluded that the Mw decreased with increasing MABz feeding dose, and the preferred reaction temperature and time were 130 °C and 48 h, respectively. After hydrogenolysis, the Mw increased slightly due to the inter- or intra-molecular hydrogen bond. TEM measurement was employed to investigate the morphologies of the nanospheres formed from the protected and de-protected copolymers (K). The results of TEM measurement showed that the nanosphere formed from the de-protected copolymer had an incompact core, and its size was smaller than that of the nanosphere formed from the protected copolymer. In the degradation experiments, faster degradation rate was accompanied with higher MA content; two fast degradation periods were observed during the degradation of samples (J and K).

Acknowledgements This work was supported by State Key Fundamental R&D Project (no. 2005CB23904), Chinese Education Ministry Foundation for Nankai University and Tianjin University Joint Academy and Trans-Century Training Program Foundation for the Talents by the Ministry of Education.

References

1. Hoste K, Schacht E, Seymour L (2000) J Control Release 64:53
2. Matsumoto S, Yamamoto A, Takakura Y, Hashida M, Tanigawa N, Sezaki H (1986) Cancer Res 46:4463
3. Vansteenkiste S, De Marre A, Schacht E (1992) J Bioact Compat Polym 7:4
4. Franssen EJF, Moolenaar F, De Zeeuw D, Meijer DKF (1994) Adv Drug Deliv Rev 14:67
5. Yokoyama M, Okano T, Sakurai Y, Ekimoto H, Shibazaki C, Kataoka K (1991) Cancer Res 51:3229
6. Shen WC, Ryser HJP (1981) Biochem Biophys Res Commun 102:1048
7. Kratz F, Beyer U, Schütte MT (1999) Crit Rev Ther Drug Carr Syst 16:245
8. Hans M, Shimoni K, Danino D, Siegel SJ, Lowman A (2005) Biomacromolecules 6:2708
9. Liang HF, Yang TF, Huang CT, Chen MC, Sung HW (2005) J Control Release 105:213
10. Cavalier M, Benoit JP, Thies C (1986) J Pharm Pharmacol 38:249
11. Holland SJ, Tighe BJ, Gould PL (1986) J Control Release 4:155
12. Cohn D, Younes H (1988) J Biomed Mater Res 22:993
13. Sawhney AS, Hubbell JA (1990) J Biomed Mater Res 24:1397

14. Zhu KJ, Song BH, Yang SL (1989) J Polym Sci A Polym Chem 27:2151
15. Chen X, McCarthy SP, Gross RA (1997) Macromolecules 30:4295
16. Pitt CG, Jeffcoat AR, Zweidinger RA, Schindler A (1979) J Biomed Mater Res 13:497
17. Schankenraad JM, Nieuwenhuis P, Molenaar I, Helder J, Dijksta PJ, Feijen J (1989) J Biomed Mater Res 23:1271
18. Barrera DA, Zylstra E, Lansbury PT, Langer R (1995) Macromolecules 28:425
19. Barrera DA, Zylstra E, Lansbury PT, Langer R (1993) J Am Chem Soc 115:11010
20. Park TG, Cohen S, Langer R (1992) Macromolecules 25:116
21. Kumar R, Gao W, Gross RA (2002) Macromolecules 35:6835
22. He B (2003) Polymer 44:989
23. He B, Wan YQ, Bei JZ, Wang SG (2004) Biomaterials 25:5239
24. Kwon GS, Kataoka K (1995) Adv Drug Deliv Rev 16:295
25. Allen C, Maysinger D, Eisenberg A (1999) Colloids Surf B Biointerfaces 16:3
26. Kabanov AV, Alakhov VY (2002) Crit Rev Ther Drug Carr Syst 19:1
27. Torchilin VP (1999) Colloids Surf B Biointerfaces 16:305
28. Wilhelm M, Zhao CL, Wang YC, Xu RL, Winnik MA et al (1991) Macromolecules 24:1033
29. Kwon GS, Naito M, Yokoyama M, Okano T, Sakurai Y, Kataoka K (1993) Langmuir 9:945
30. Trimaille T, Pichot C, Elaissari A, Fessi H, Briancon S, Delair T (2003) Colloid Polym Sci 281:1184
31. Tobio M, Gref R, Sanchez A, Langer R, Alonso MJ (1998) Pharm Res 15:27033
32. Zhang Y, Zhang Q, Zha L, Yang W, Wang C, Jiang X, Fu S (2004) Colloid Polym Sci 282:1323
33. Deng X, Liu Y, Yuan M (2002) Eur Polym J 38:1435
34. Guerin P, Vert M, Braud C, Lenz RW (1985) Polym Bull (Berl) 14:187
35. Coulembier O, Degee P, Gerbaux P, Wantier P, Barbaud C, Flammang R, Guerin P, Dubois P (2005) Macromolecules 38:3141
36. Fietier I, Le Borgne A, Spassky N (1990) Polym Bull (Berl) 24:349
37. Zhou QX, Kohn J (1990) Macromolecules 23:3399
38. Cammas S, Renard I, Langlois V, Guerin P (1996) Polymer 37:4215
39. Kricheldorf HR, Kreiser-Saunders I, Stricker A (2000) Macromolecules 33:702
40. Kowalski A, Duda A, Penczek S (2000) Macromolecules 33:7359
41. Duda A, Kowalski A, Libiszowski J, Penczek S (2005) Macromol Symp 224:71
42. Dobrzynski P, Kasperczyk J, Janeczek H, Bero M (2001) Macromolecules 34:5090
43. Hiltunen K, Harkonen M, Seppala JV, Vaananen T (1996) Macromolecules 29:8677–8682
44. Tuominen J, Seppala JV (2000) Macromolecules 33:3530
45. Boutault K, Cammas S, Huet F, Guerin P (1995) Macromolecules 28:3516